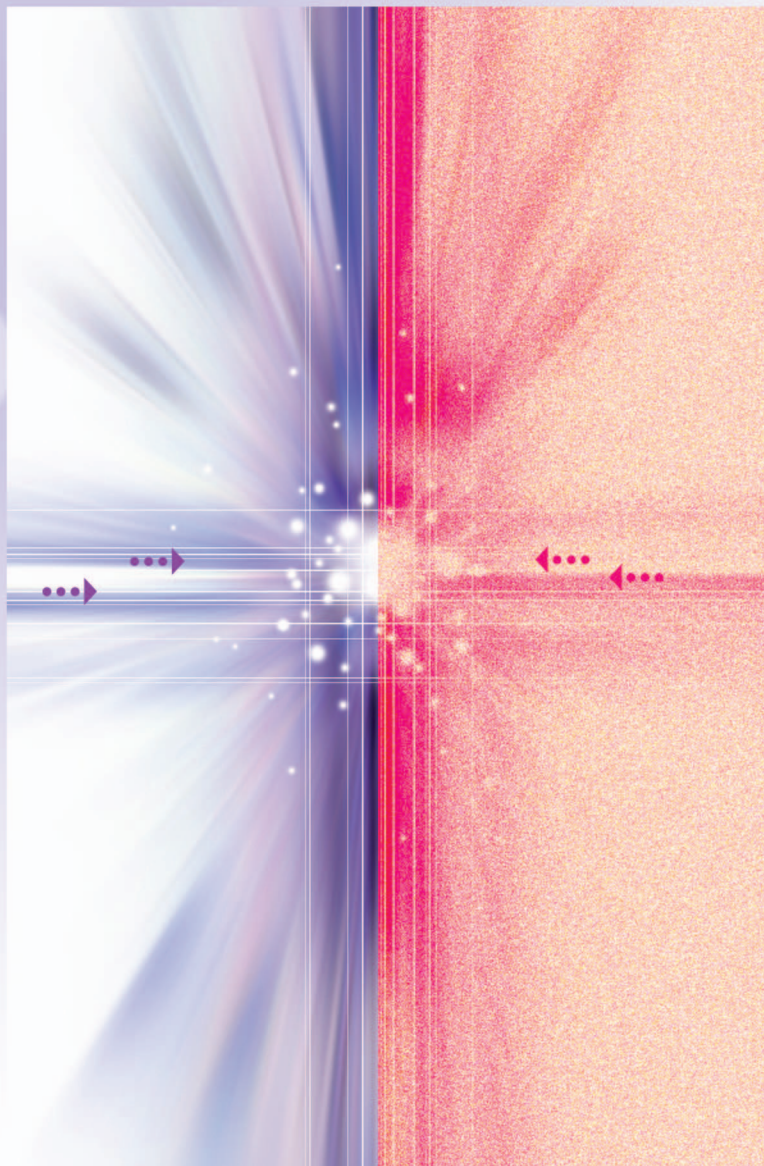


Combining Coarse and Fine Models for Optimal Design

*Qingsha S. Cheng,
John W. Bandler, and
Slawomir Koziel*

Since the space mapping concept [1], [2] was first developed, it has been successfully applied to microwave engineering design problems as well as in other engineering fields (e.g., [3], [4]). In the meantime, much research has been carried out on various space mapping and related approaches [5]–[8]. Space mapping has also been combined with formulations such as neural networks [9]. Among the developments in the art of space mapping, implicit space mapping [10] is probably the simplest technique to implement. Here, no matrix calculation is needed. It can be generalized to include all other forms of space mapping in a generalized implicit space mapping framework [5].



© IMAGESTATE

Qingsha S. Cheng (chengq@mcmaster.ca), John W. Bandler, and Slawomir Koziel are with the Simulation Optimization Systems Research Laboratory, Department of Electrical and Computer Engineering, McMaster University, Hamilton, Ontario, Canada. John W. Bandler is also with Bandler Corporation, Dundas, Ontario, Canada.

Digital Object Identifier 10.1109/MMM.2007.910950

In both the fine model and corresponding coarse models, certain preassigned parameters exist; for example, dielectric constant and the height of the substrate.

In the microwave arena, circuit-theory based CAD tools such as Agilent ADS [11] are fast and easy to use for design optimization. On the other hand, electromagnetic (EM) simulators such as Agilent Momentum, Sonnet *em* [12], Ansoft HFSS [13], or FEKO [14] are usually CPU-intensive but offer high-fidelity validations. Implicit space mapping is a simple approach to combine a circuit-theory based CAD model, or “coarse” model, and an EM simulator, or “fine” model, to achieve fast and accurate optimal design and modeling.

In both the fine model and corresponding coarse models, certain preassigned parameters exist; for example, dielectric constant and the height of the substrate. They are normally selected and their values fixed early in the modeling and design process. Implicit space mapping explores the flexibility of these parameters in the design optimization [10] and device modeling [15] tasks. The effects on the responses of microwave components of varying the values of these parameters may be as significant as those achieved by varying the optimizable parameters. In our space mapping technique, we apply this flexibility to the coarse model only.

Thus, we calibrate certain selected coarse model pre-assigned parameters in each space mapping iteration to match the response of the fine model. With these re-calibrated preassigned parameters now fixed in value, the enhanced coarse model (surrogate) is then re-optimized to obtain a new design. We apply this new design to the fine model. These steps are repeated until the design specification is satisfied.

Generally speaking, the coarse model could be implemented using any circuit simulator. In our examples, coarse models are realized in Agilent ADS. We use Sonnet *em* and FEKO as the fine model evaluators. Agilent ADS schematics organize the ADS optimization engine and coarse and fine models to perform parameter extraction (obtain a mapping to re-match the models) and surrogate optimization (obtain a new prediction of the desired optimal solution). Figure 1 illustrates the relationship between the models and simulators.

Space mapping belongs to the category of surrogate-based optimization approaches. There is a rich literature concerning surrogate-based optimization. In [16], the authors describe so-called approximation and model management optimization. This approach assumes that the surrogate model satisfies so-called zero- and first-order consistency conditions with the high-fidelity model in question. A surrogate management framework and its applications for engineering design are presented in [17]. Surrogate optimization based on kriging

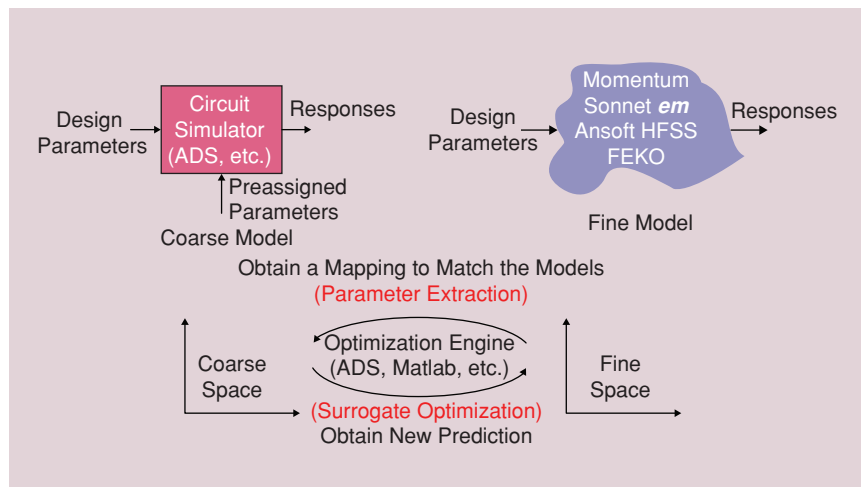


Figure 1. Space mapping implementation concept.

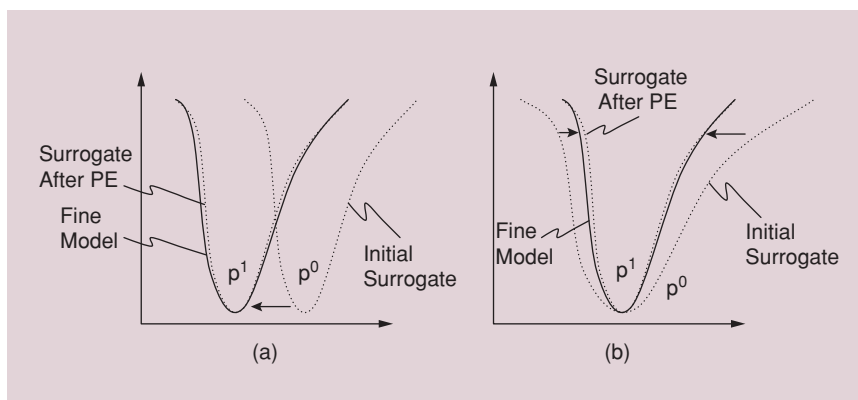


Figure 2. Two illustrations of parameter extraction (PE) for matching the initial surrogate (coarse model) to the fine model. The initial surrogate and fine model deviate from each other at the initial iteration. After the parameter extraction process, preassigned parameter p^0 becomes p^1 , and the new surrogate model is aligned with the fine model. We show two cases. In (a), the surrogate model is shifted to match the fine model as the preassigned parameter vector changes from p^0 to p^1 . In (b), the surrogate model is squeezed to match the fine model as the preassigned parameter vector changes from p^0 to p^1 .

The Implicit Space Mapping Concept [10], [21]

Our goal is to design a fine model optimal solution

$$\mathbf{x}^* = \arg \min_{\mathbf{x}} U(\mathbf{R}_f(\mathbf{x})) \quad (1)$$

Here, the fine-model response vector is denoted by \mathbf{R}_f , e.g., $|\mathbf{S}_{11}|$ at selected frequency points. The fine-model design parameters are denoted \mathbf{x} . U is a suitable objective function. In microwave engineering, U is typically a minimax objective function with upper and lower specifications [22]; \mathbf{x}^* is the optimal design to be determined. Implicit space mapping uses the following iterative procedure to solve (1)

$$\mathbf{x}^{k+1} = \arg \min_{\mathbf{x}} U(\mathbf{R}_c(\mathbf{x}, \mathbf{p}^k)) \quad (2)$$

where $\mathbf{R}_c(\mathbf{x}, \mathbf{p})$ is a response vector of the coarse model with \mathbf{x} and \mathbf{p} being the design variables and preassigned parameters, respectively. $\mathbf{R}_c(\mathbf{x}, \mathbf{p}^k)$ is an implicit space mapping surrogate model with preassigned parameters \mathbf{p}^k obtained at iteration k using the parameter extraction procedure

$$\mathbf{p}^k = \arg \min_{\mathbf{p}} \|\mathbf{R}_f(\mathbf{x}^k) - \mathbf{R}_c(\mathbf{x}^k, \mathbf{p})\| \quad (3)$$

in which we try to match the surrogate to the fine model. The initial surrogate model is $\mathbf{R}_c(\mathbf{x}, \mathbf{p}^0)$, where \mathbf{p}^0 represents the initial preassigned parameter values. In other words, the surrogate model is the coarse model with updated values of the preassigned parameters.

models are discussed in [18]. A survey of surrogate-based analysis and optimization methods is given in [19]. It should be emphasized that a characteristic feature that differentiates space mapping from some other surrogate-based optimization methods is that in our space mapping approach the surrogate model is constructed using an available, low-fidelity (and physically meaningful) model of the object response (the model being a function of the actual design variables), rather than a pure interpolation or approximation.

There are many other approaches that aim at reducing the total time cost of fine model evaluations, such as the model order reduction (MOR) method. The MOR method [20] is a way of reducing unnecessary complexity in a system in order to obtain a faster-to-compute model. It is a bottom-up approach, since it considers the details of the fine model and attempts to reduce its order. However, space mapping works top-down. It tries to reconcile two existing models, a coarse model with a fine model, even without the implementation details of the fine model. MOR aims at reducing the fine model's complexity, while space mapping aims at minimizing the number of calls to the fine model.

Implicit Space Mapping

The formulation of the implicit space mapping algorithm is presented in the sidebar (see "The Implicit Space Mapping Concept") [10], [21]. Our goal is to obtain the fine model optimal design without going to direct optimization of the fine model but instead using the surrogate model; i.e., the coarse model with updated values of the preassigned parameters. Parameter extraction and design optimization are performed solely on the surrogate model. A prediction of the next fine model design is also obtained through the surrogate.

We illustrate the space mapping process in Figure 2. In this illustration, the solid lines are the fine model representations and the dotted lines are the

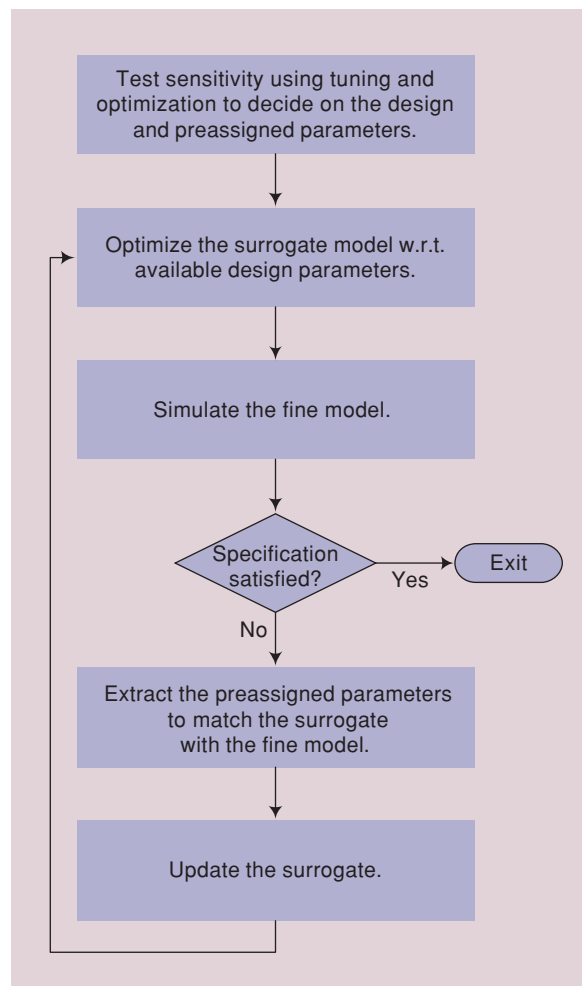


Figure 3. Implicit space mapping algorithm flowchart [10], [21].

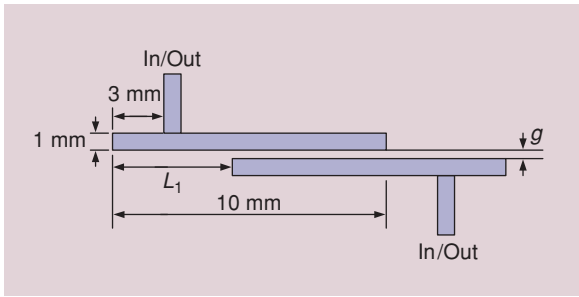


Figure 4. Geometry of the second-order tapped-line microstrip filter [23].

surrogates. In both cases, the selected preassigned parameters p^1 are extracted such that the surrogate is closely matched to the fine model. After the extraction, the new surrogate replaces the fine model, becoming the function to be optimized. The solution is our new fine model solution. We can then simulate the fine model for verification of its response. If the fine model design specification is not satisfied, the steps can be repeated. Please refer to the sidebar for a formal description of the implicit space mapping technique. We summarize the implicit space mapping algorithm in the flowchart of Figure 3.

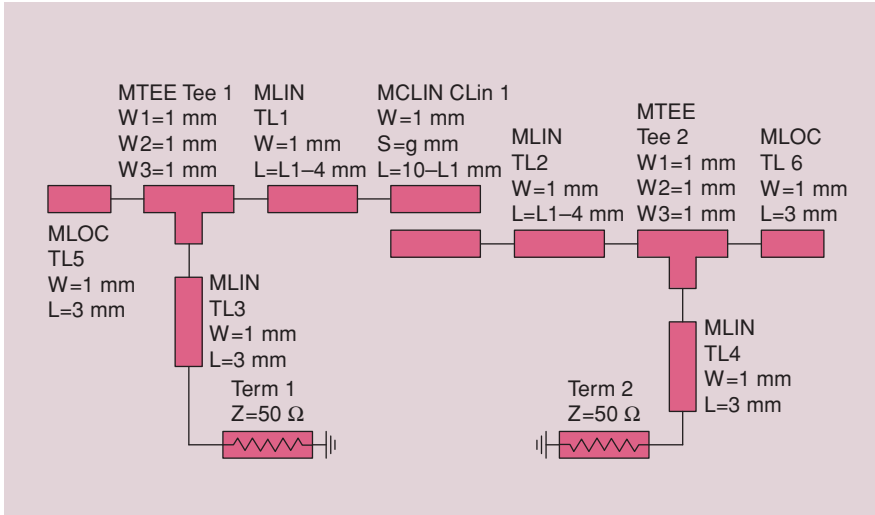


Figure 5. Coarse model of the second-order tapped-line microstrip filter (Agilent ADS).

Tapped-Line Microstrip Filter Illustration

We now demonstrate the implicit space mapping technique on a simple optimization problem, the second-order tapped-line microstrip filter [23] shown in Figure 4.

For the sake of simplicity we only use two design parameters, L_1 and g as defined in Figure 4. The fine model is simulated in FEKO [14]. The design specifications are $|S_{21}| \geq -3$ dB for $4.75 \text{ GHz} \leq \omega \leq 5.25 \text{ GHz}$, and $|S_{21}| \leq -20$ dB for 3.0

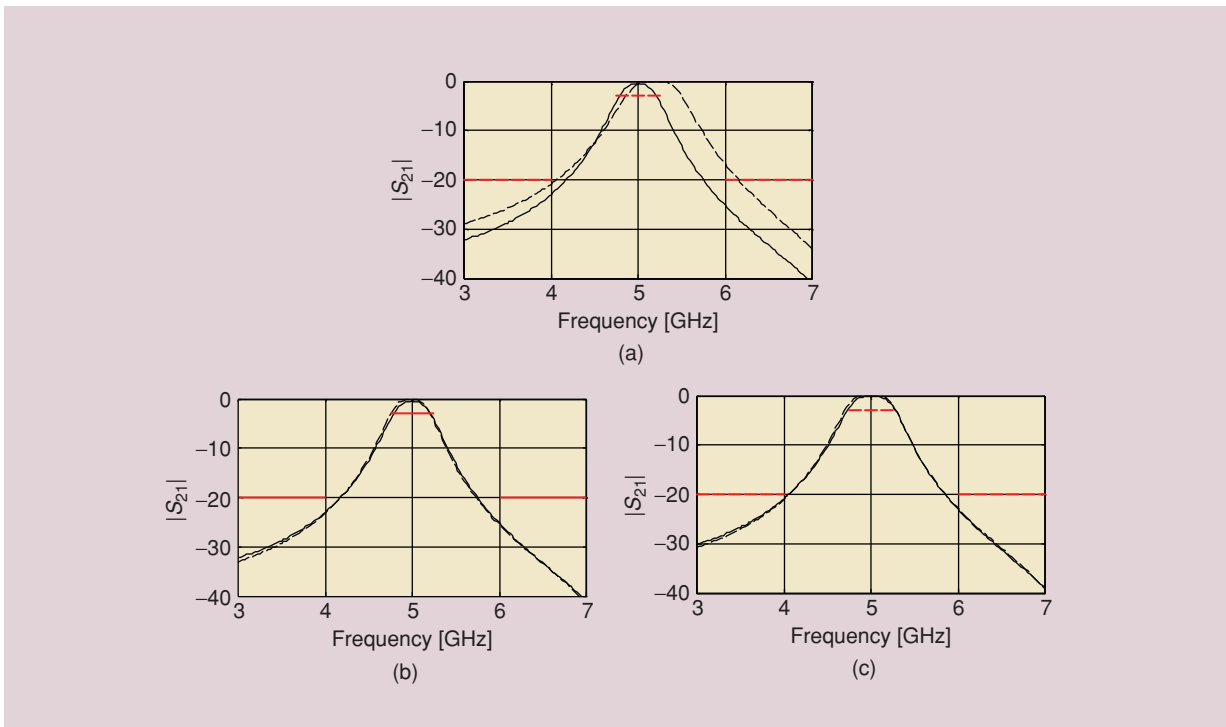


Figure 6. Second-order tapped-line microstrip filter responses: fine model (—) versus coarse model (---). (a) Initial design. (b) A good match is obtained after extracting the preassigned parameters. (c) A good fine model response is obtained in just two iterations.

$\text{GHz} \leq \omega \leq 4.0 \text{ GHz}$ and $6.0 \text{ GHz} \leq \omega \leq 7.0 \text{ GHz}$. The coarse model shown in Figure 5 is the circuit equivalent of the structure in Figure 4 and is implemented in Agilent ADS [11].

We want to optimize our filter using implicit space mapping with the dielectric constant ϵ_r and the height H of the substrate as tuning parameters. Initial values of the parameters are 9.9 and 100 mils, respectively, for both fine and coarse models. These parameters remain fixed in the fine model; however, we are going to tune them in the coarse model, according to the implicit space mapping methodology.

The initial design, $L_1 = 6.977 \text{ mm}$ and $g = 0.060 \text{ mm}$, is the optimal solution of the coarse model with respect to our specifications. Figure 6(a) shows the fine and coarse model responses at the initial design. Note that neither the coarse nor fine models satisfy the design specifications. Also, there is quite a significant misalignment between the fine and coarse models both with respect to center frequency and bandwidth. We now perform the parameter extraction procedure. Figure 6(b) shows the fine model and surrogate model (i.e., the tuned coarse model) response at the initial design. We (re)optimize the design parameters in our surrogate with the newly obtained

Implicit space mapping is a simple approach to combine a circuit-theory based CAD model and an EM simulator model to achieve fast and accurate optimal design and modeling.

preassigned parameter values. A new set of design parameter values is found to supply to fine model. In this manner, we obtain a good fine model design in just two iterations [Figure 6(c)].

For comparison purposes we also perform the direct optimization of the fine model using Matlab [24]. It turns out that the implicit space mapping

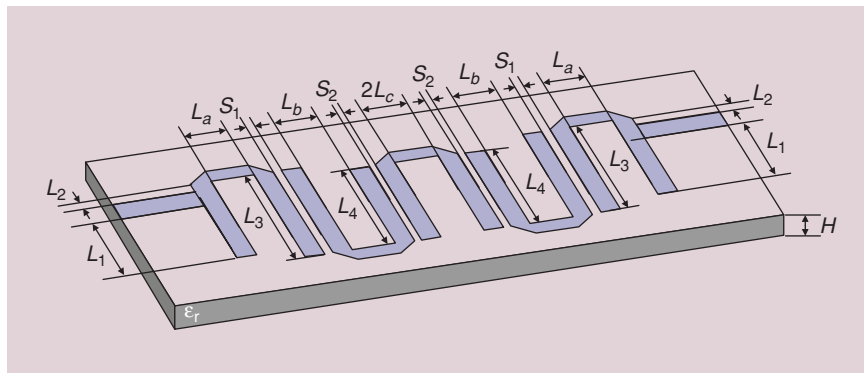


Figure 7. The microstrip hairpin filter [25].

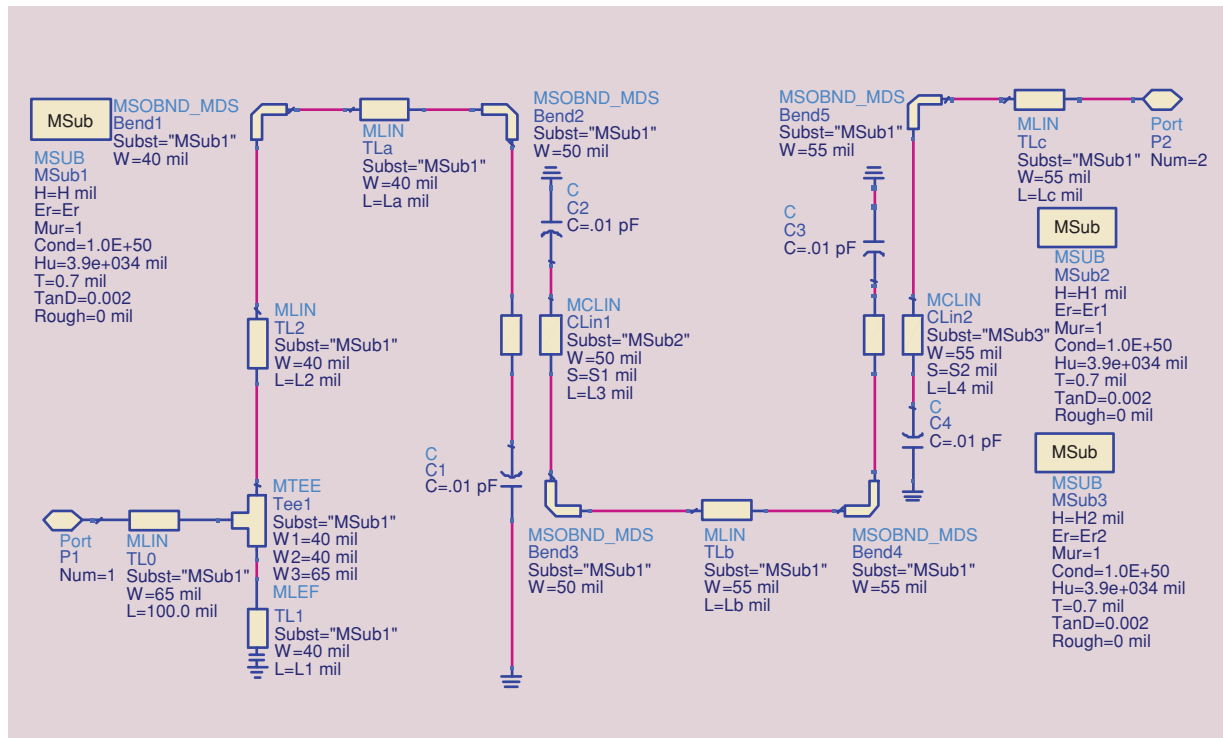


Figure 8. A microstrip hairpin filter is “half” implemented, since the structure is symmetric.

The implicit space mapping optimization of our filter, which takes only 17 minutes, is substantially faster than the direct optimization, which requires 4.5 hours.

optimization of our filter, which requires only three evaluations of the fine model (plus a small overhead related to parameter extraction and optimization of the surrogate model), takes only about 17 minutes. This is substantially faster than the direct optimization, which requires 54 fine model evaluations and takes about 4.5 hours.

Microstrip Hairpin Filter Design

We now describe in detail the design process of the microstrip hairpin filter [25] example of Figure 7, where the implicit space mapping algorithm, including the coarse/surrogate model evaluation, is implemented in Agilent ADS. The fine model responses are loaded from the result of an external EM simulator using the ADS SnP file. In three iterations, we have a

Sonnet *em* design with much better performance than reported in [25].

We use the original design specifications of [25]: $|S_{11}| < -16$ dB for $3.7 \text{ GHz} \leq \omega \leq 4.2 \text{ GHz}$; $|S_{21}| < -28$ dB for $\omega \leq 3.2 \text{ GHz}$ and $\omega \geq 4.7 \text{ GHz}$.

Our coarse model is the same ADS circuit model as in [25]. A “half filter” is implemented in ADS, as shown in Figure 8. The two half-filters are connected in a “back-to-back” fashion [25]. We use L_1, L_2, L_3, L_4, S_1 , and S_2 , as design parameters. An ADS test optimization and tuning process show that if we add L_c to the set of design parameters, the flexibility will improve the performance of the filter. The test also shows that L_2 should be set to a small value. So we fix L_2 to zero. The design variable set now becomes L_1, L_3, L_4, S_1, S_2 , and L_c . We implement a coarse model optimization schematic in Figure 9. The coarse model is capable of obtaining a better passband performance than the original design specification. We then tighten the specification to $|S_{11}| < -40$ dB for the passband and $|S_{21}| < -30$ dB for the stopband.

In Figure 10, the ADS test shows that the specification is easily satisfied. To compensate for the design parameter value changes, we use a set of preassigned parameters. The uniform dielectric constant ϵ_r and

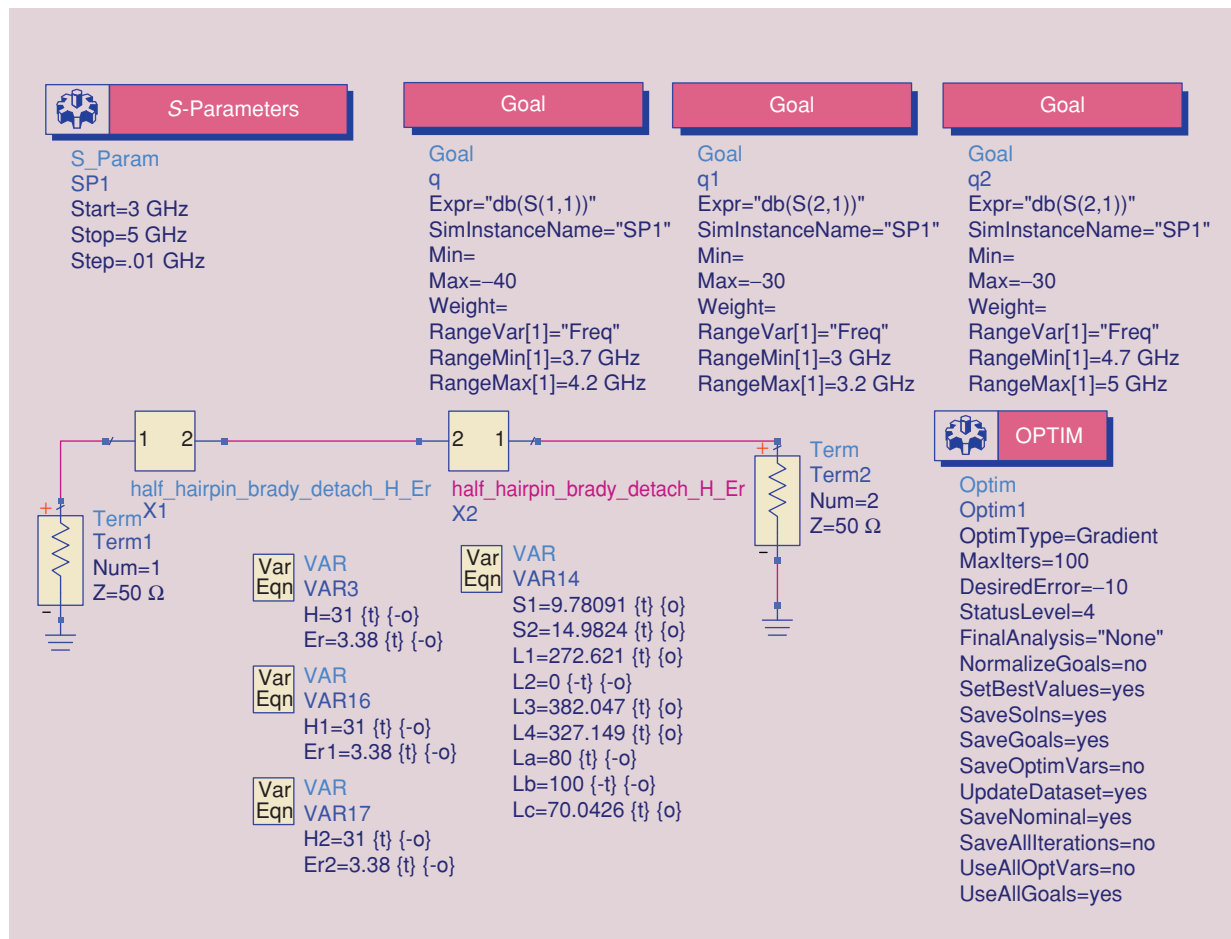


Figure 9. The coarse (surrogate) model optimization process implemented in Agilent ADS.

substrate height H are not sufficient to compensate for the changes in the design parameters. We introduce different dielectric constants ϵ_{r1} and ϵ_{r2} , and substrate height H_1 and H_2 for the coupled lines "CLin1" and "CLin2," respectively, as annotated in Figure 8 (substrate components MSub2 and MSub3 are assigned to CLin1 and CLin2, respectively; MSub1 is assigned to the rest of the microstrip components).

In the fine model, we use Sonnet *em* with a very fine cell size of 1 mil \times 1 mil (see Figure 11 and Figure 12). Each frequency point takes about 50 minutes to complete on a Pentium 4 with 3.4 GHz CPU and 2 GB RAM. Total simulation time for a 25-frequency-point sweep is around 17 hours.

One of the most important steps, parameter extraction, is implemented entirely in ADS (Figure 13). The fine model solution is imported from a Touchstone file generated by Sonnet *em*. The surrogate optimization is implemented by ADS in exactly the same way as in Figure 9 but with different preassigned parameter values for each iteration.

In the initial iteration, we use an adaptive frequency sweep, since it is shifted away from the specification as seen in Figure 14. (The passband details are not important at this stage.) The first iteration shifts the responses back to the desired frequency bands

In the fine model, we use Sonnet *em* with a very fine cell size of 1 mil \times 1 mil.

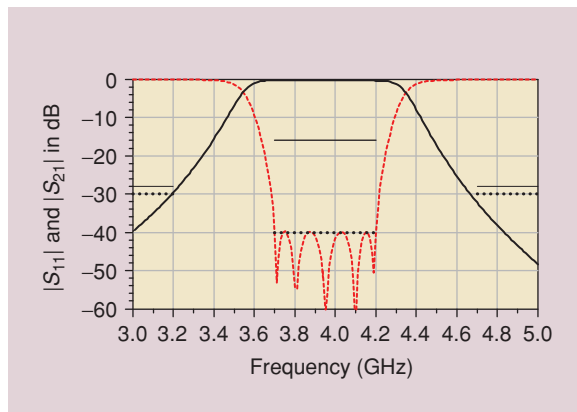


Figure 10. Coarse model optimal responses $|S_{11}|$ (---) and $|S_{21}|$ (—); the desired specification [25] (—) and the tightened specification (...).

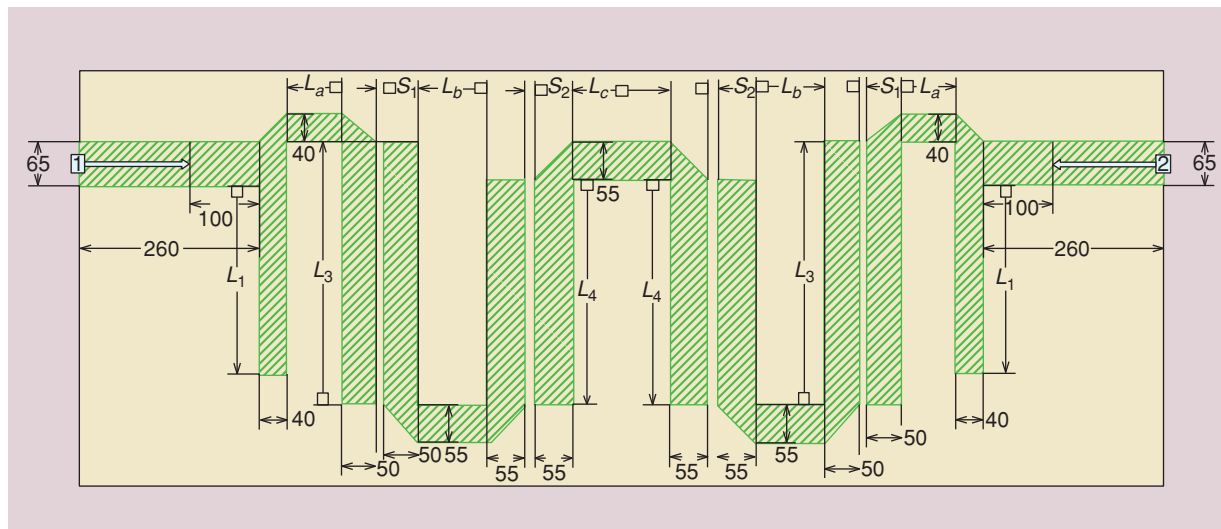


Figure 11. The fine model implementation in Sonnet *em*.

(Figure 15). We conducted a fine frequency sweep in the passband region. The second iteration finds a good solution without much difficulty (Figure 16). The third iteration fine tunes the responses. A return loss of -34 dB in the passband is obtained, as shown in Figure 17. In Table 1 we list the parameter values of the initial and the final designs.

The solution reported in Table 1 can be further improved by performing one iteration of a space mapping algorithm using the so-called output space

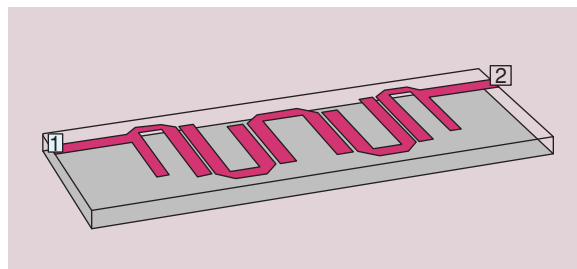


Figure 12. The fine model in Sonnet *em*: a three-dimensional view.

mapping surrogate model, which allows us to ensure a perfect match with the fine model at the current iteration point [5]. The improved solution is $L_1 = 280$, $L_3 = 448$, $L_4 = 342$, $S_1 = 9$, $S_2 = 12$, $L_c = 86$ (dimensions in mil), and the corresponding fine model response is shown in Figure 18.

Discussion

Our design starts from Brady's back-to-back ADS design [25]. In his paper [25], the author probably expected a narrower passband from the Sonnet *em* simulation and the test fabrication, so he applied a wider bandwidth for the passband in the ADS circuit

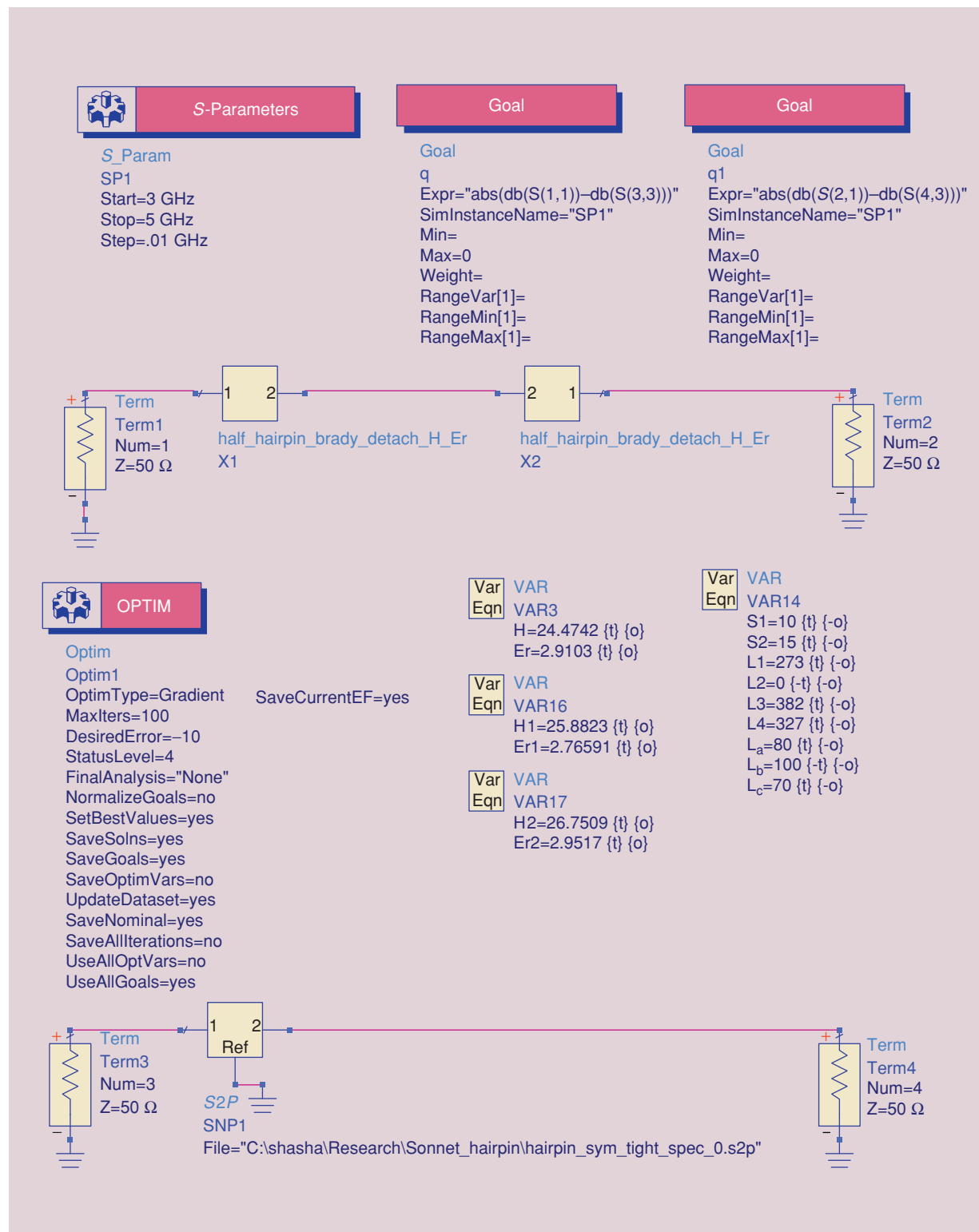


Figure 13. The parameter extraction process implemented in Agilent ADS.

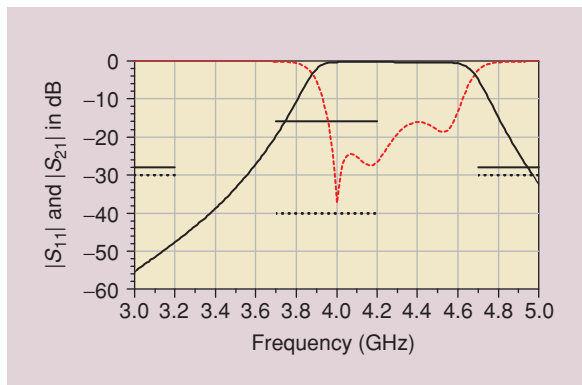


Figure 14. Fine model responses $|S_{11}|$ (---) and $|S_{21}|$ (—) at the initial solution, the desired specification [25] (—), and the tightened specification (...).

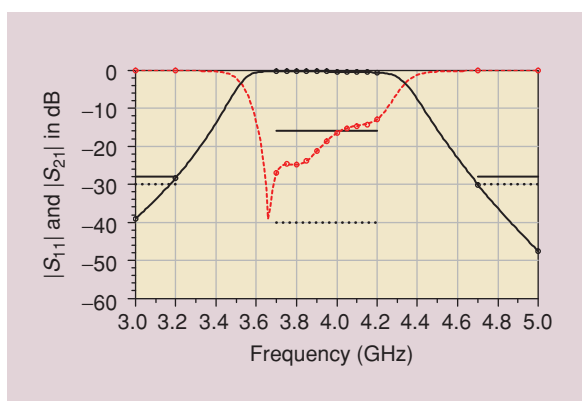


Figure 15. Fine model responses $|S_{11}|$ (---) and $|S_{21}|$ (—) after the first iteration, the desired specification [25] (—), and the tightened specification (...).

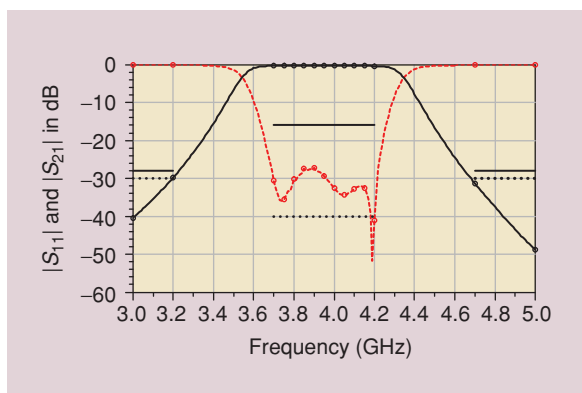


Figure 16. Fine model responses $|S_{11}|$ (---) and $|S_{21}|$ (—) after the second iteration, the desired specification [25] (—), and the tightened specification (...).

simulator (coarse model) optimization specification; i.e., the passband is changed to $3.55 \text{ GHz} \leq \omega \leq 4.4 \text{ GHz}$ from $3.7 \text{ GHz} \leq \omega \leq 4.2 \text{ GHz}$.

However, the trade-off is that the increased bandwidth deteriorates the passband performance. When the ADS design is applied to Sonnet *em*, the specifica-

TABLE 1. Microstrip hairpin filter design parameter values.

Design Variables	Initial Design (mil) (Coarse Model Optimal Design)	Final On-Grid Design (mil)
L_1	273	280
L_3	382	448
L_4	327	341
S_1	10	9
S_2	15	12
L_c	70	87

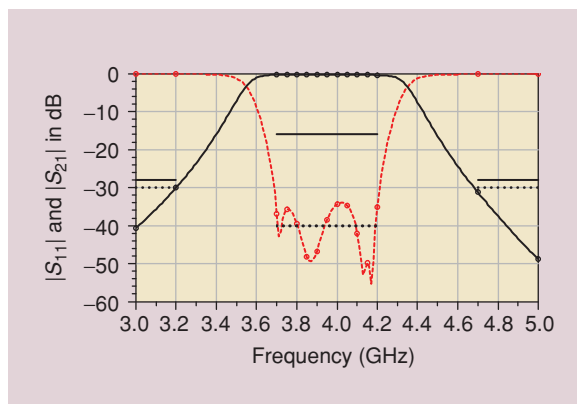


Figure 17. Fine model responses $|S_{11}|$ (---) and $|S_{21}|$ (—) after the third iteration, the desired specification [25] (—), and the tightened specification (...).

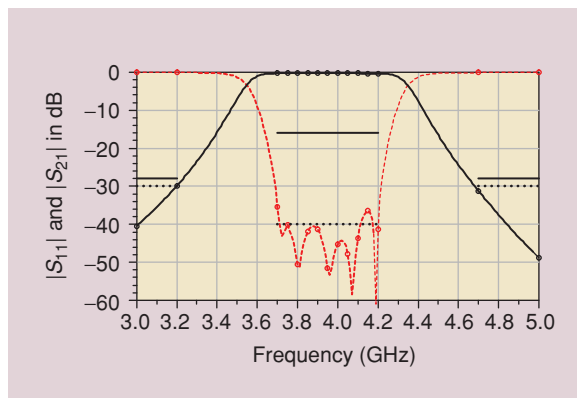


Figure 18. Fine model responses $|S_{11}|$ (---) and $|S_{21}|$ (—) at the final solution improved by one space mapping iteration with an output space mapping surrogate model, the desired specification [25] (—), and the tightened specification (...).

tion is barely satisfied, while the bandwidth is much wider than necessary. Space mapping uses a parameter extraction procedure in each iteration. The parameter extraction procedure “absorbs” the difference between the Sonnet *em* model and the ADS model. Therefore, we can keep the desired specification as our coarse

Space mapping uses a parameter extraction procedure in each iteration, which “absorbs” the difference between the Sonnet *em* model and the ADS model.

model or surrogate optimization specification. With a proper choice of design parameters, we can even use the tightened design specifications and thus obtain a better Sonnet *em* design.

Summary

In this article we reviewed the implicit space mapping concept. We illustrated it using a simple tapped-line microstrip filter example. We demonstrated the robustness of our approach by performing an accurate design of a microstrip hairpin filter. A detailed and easy-to-follow design optimization procedure was provided and the Agilent ADS implementation of the algorithm was described. A good electromagnetically validated design in Sonnet *em* was obtained in a few fine model simulations.

Acknowledgments

This work was supported in part by the Natural Sciences and Engineering Research Council of Canada under Grants RGPIN7239-06, STPGP336760-06 and by Bandler Corporation. We thank Sonnet Software, Inc., for *em*, EM Software & Systems-S.A. (Pty) Ltd. for FEKO, and Agilent Technologies for ADS. We also thank the reviewers for their constructive suggestions.

References

- [1] J.W. Bandler, R.M. Biernacki, S.H. Chen, P.A. Grobelny, and R.H. Hemmers, “Space mapping technique for electromagnetic optimization,” *IEEE Trans. Microwave Theory Tech.*, vol. 42, no. 12, pp. 2536–2544, Dec. 1994.
- [2] J.W. Bandler, Q.S. Cheng, S.A. Dakrouy, A.S. Mohamed, M.H. Bakr, K. Madsen, and J. Søndergaard, “Space mapping: The state of the art,” *IEEE Trans. Microwave Theory Tech.*, vol. 52, no. 1, pp. 337–361, Jan. 2004.
- [3] M. Redhe and L. Nilsson, “Using space mapping and surrogate models to optimize vehicle crashworthiness design,” in *Proc. 9th AIAA/ISSMO Multidisciplinary Analysis Optimization Symp.*, Atlanta, GA, Sep. 2002, paper AIAA 2002-5536.
- [4] G. Crevecoeur, L. Dupre, and R. Van de Walle, “Space mapping optimization of the magnetic circuit of electrical machines includ-

- ing local material degradation,” *IEEE Trans. Magn.*, vol. 43, no. 6, pp. 2609–2611, June 2007.
- [5] S. Koziel, J.W. Bandler, and K. Madsen, “A space-mapping framework for engineering optimization—Theory and implementation,” *IEEE Trans. Microwave Theory Tech.*, vol. 54, no. 10, pp. 3721–3730, Oct. 2006.
- [6] J.C. Rautio, “A space mapped model of thick, tightly coupled conductors for planar electromagnetic analysis,” *IEEE Microwave Mag.*, vol. 5, no. 3, pp. 62–72, Sept. 2004.
- [7] D.G. Swanson Jr. and R.J. Wenzel, “Fast analysis and optimization of combine filters using FEM,” in *IEEE MTT-S Int. Microwave Symp. Dig.*, Phoenix, AZ, pp. 1159–1162, June 2001.
- [8] A. Pavia, L. Zhao, R. Lucero, and J. Estes, “Optimization of multi-layer circuits using companion models and space mapping,” presented at *Workshop on Microwave Component Design Using Optimization Techniques*, IEEE MTT-S Int. Microwave Symp., Philadelphia, PA, 2003.
- [9] J.E. Rayas-Sánchez and V. Gutiérrez-Ayala, “EM-based Monte Carlo analysis and yield prediction of microwave circuits using linear-input neural-output space mapping,” *IEEE Trans. Microwave Theory Tech.*, vol. 54, no. 12, pp. 4528–4537, Dec. 2006.
- [10] J.W. Bandler, Q.S. Cheng, N.K. Nikolova, and M.A. Ismail, “Implicit space mapping optimization exploiting preassigned parameters,” *IEEE Trans. Microwave Theory Tech.*, vol. 52, no. 1, pp. 378–385, Jan. 2004.
- [11] Agilent Advanced Design System (ADS), ver. 2005A, Agilent Technologies, Santa Rosa, CA, 2005.
- [12] Sonnet *em*, ver. 11.52, Sonnet Software, North Syracuse, NY, 2007.
- [13] Ansoft High Frequency Structure Simulator (HFSS), ver. 10, Ansoft Corporation, Pittsburgh, PA, 2006.
- [14] FEKO® *User’s Manual*, Suite 4.2, EM Software & Systems-S.A. (Pty) Ltd, Stellenbosch, South Africa, 2004.
- [15] Q.S. Cheng and J.W. Bandler, “An implicit space mapping technique for component modeling,” in *Proc. 36th European Microwave Conf.*, Manchester, UK, pp. 458–461, Sept. 2006.
- [16] N.M. Alexandrov and R.M. Lewis, “An overview of first-order model management for engineering optimization,” *Optimization Eng.*, vol. 2, no. 4, pp. 413–430, 2001.
- [17] A.L. Marsden, M. Wang, J.E. Dennis, and P. Moin, “Optimal aeroacoustic shape design using the surrogate management framework,” *Optimization Eng.*, vol. 5, no. 2, pp. 235–262, 2004.
- [18] S.E. Gano, J.E. Renaud, and B. Sanders, “Variable fidelity optimization using a kriging based scaling function,” in *Proc. 10th AIAA/ISSMO Multidisciplinary Analysis and Optimization Conf.*, Albany, NY, Aug. 2004, paper AIAA 2004-4460.
- [19] N.V. Queipo, R.T. Haftka, W. Shyy, T. Goel, R. Vaidynathan, and P.K. Tucker, “Surrogate-based analysis and optimization,” *Prog. Aerosp. Sci.*, vol. 41, no. 1, pp. 1–28, 2005.
- [20] R. Achar and M.S. Nakhla, “Simulation of high-speed interconnects,” *Proc. IEEE*, vol. 89, no. 5, pp. 693–728, May 2001.
- [21] Q.S. Cheng, J.W. Bandler, and J.E. Rayas-Sánchez, “Tuning-aided implicit space mapping,” *Int. J. RF Microwave Computer-Aided Eng.*, to be published.
- [22] J. Zhu, J.W. Bandler, N.K. Nikolova, and S. Koziel, “Antenna optimization through space mapping,” *IEEE Trans. Antennas Propag.*, vol. 55, no. 3, pp. 651–658, Mar. 2007.
- [23] A. Manchec, C. Quendo, J.-F. Favennec, E. Rius, and C. Person, “Synthesis of capacitive-coupled dual-behavior resonator (CCDBR) filters,” *IEEE Trans. Microwave Theory Tech.*, vol. 54, no. 6, pp. 2346–2355, June 2006.
- [24] Matlab, Version 7.1, The MathWorks, Inc., Natick, MA, 2005.
- [25] D. Brady, “The design, fabrication and measurement of microstrip filter and coupler circuits,” *High Freq. Electronics*, vol. 1, no. 1, pp. 22–30, July 2002.

